

# Comprehensive assessment of the climate-induced water scarcity over continental Chile

Francisco Zambrano<sup>a,1,1,\*</sup>, Bob Security<sup>b</sup>, Cat Memes<sup>b,2</sup>, Derek Zoolander<sup>1,2</sup>

<sup>a</sup>*Facultad de Ciencias, Universidad Mayor., La Piramide 5750, Santiago, 123456, Huechuraba, United States*

<sup>b</sup>*Department, A street 29, Manchester., 2054 NX, The Netherlands*

---

## Abstract

Human-induced greenhouse gas emissions have increased the frequency and/or intensity of some weather and climate extremes globally. Chile has been affected by persistent water scarcity which is impacting the hydrological system and vegetation development. Central Chile it is been the focus of research studies due to the diminishing water supply, nevertheless our results evidence that water deficit is expanded beyond. We analyze earth observation data for 2000-2023 to make a comprehensive assessment of water scarcity in Chile. For the analysis, continental Chile was divided into five zones big north, little north, central, south, and austral zone. We used the time series of MODIS for land cover change (LULC), fraction of vegetation cover (FVC), and to derive the drought index zcNDVI and zcET (standardized anomaly of cumulative NDVI and ET through the growing season); and CHELSA v2.1 dataset to derive the standardized precipitation evapotranspiration index (SPEI). We evaluate the interconnection between the productivity drought index (zcNDVI) and water demand (zcET), supply (SPEIs) and FVC. Finally, we analyzed the temporal correlation of the drought indices with total water storage (TWS) from GRACE (Gravity Recovery and Climate Experiment). Our LULC results showed a increasing trend of 412 [ $km^2 \cdot yr^{-1}$ ] of forest in the south zone, a decresasing trend of 24 [ $km^2 \cdot yr^{-1}$ ] of cropland in the central zone and an increase of 31 [ $km^2 \cdot yr^{-1}$ ] in the south zone, and a diminish of 80 [ $km^2 \cdot yr^{-1}$ ] of barrend land in the austral zone.

*Keywords:* keyword1, keyword2

---

## 1. Introduction

The sixth assessment report (AR6) of the IPCC [1] indicates that human-induced greenhouse gas emissions have increased the frequency and/or intensity of some weather and climate extremes and the evidence has been strengthened since AR5 [15]. There is high confidence that the increasing global warming can expand the land area affected by increasing drought frequency and severity [30]. Chile has been facing a persistent rainfall deficit lasting for more than ten years [14] which has impacted the hydrological system [6], and consequently the vegetation development [38].

Precipitation is the primary driver of drought that impacts hydrological regimes and vegetation productivity. Thus, it is commonly classified as meteorological, hydrological, and agricultural [35]. Lately, it has been argued that this definition does not fully address the ecological dimensions [9]. Crausbay et al. [9] proposed the ecological drought definition as “an episodic deficit in water availability that drives ecosystems beyond thresholds of vulnerability, impacts ecosystem services, and triggers feedback in natural and/or human systems”. The AR6 [1] state that even if global warming is stabilized at 1.5°-2°C many parts of the

---

\*Corresponding author

*Email addresses:* francisco.zambrano@umayor.com (Francisco Zambrano), bob@example.com (Bob Security), cat@example.com (Cat Memes), derek@example.com (Derek Zoolander)

<sup>1</sup>This is the first author footnote.

<sup>2</sup>Another author footnote.

world will be impacted by more severe agricultural and ecological drought. Central Chile has suffered from crop productivity failure, highlighting the growing season 2007-2008 and 2008-2009 [39, 40], which impacted an extensive surface. But, in 2019-2020, the drought intensity reached an extreme condition at North 34°S not seen -at least- for more than 40 years [38], affecting forest, grassland, and croplands areas. The prolonged lack of precipitation within Central Chile is producing changes in the ecosystem that must be studied.

Satellite remote sensing [34, 2] is the primary method to evaluate how meteorological drought impacts vegetation dynamics. Since the 90's multiple vegetation drought indices have been derived (VCI,[16]; TCI, [17];zNDVI, [27]; VegDri, [7]) that have allowed making spatiotemporal analysis. Although we can calculate those indices for any time during the year (depending on satellite revisit), there are relevant during the stage vegetation has more activity, the growing season [22]. Although modeling phenology is a complex task, satellites offer strategies that help to address it [37, 33, 8]. Also, the land cover dynamics product MCD12Q2 from the USGS [12] provides some phenology metrics. Some authors have proposed indices aggregated during the season. Meroni et al. [20] accumulating the fractional active photosynthetic active radiation(FAPAR) between the start (SOS) and the end of the season (EOS) in the Sahel, calculate the zCFAPAR. Zambrano et al. [40] used the same approach but with the NDVI (Normalized Difference Vegetation Index), derivating the zcNDVI within Central Chile. Besides, land use land cover (LULC) change can be driven by drought [32, 4]. To analyze those changes, multiple time-series LULC products exist as the MCD12Q1 [12] and the ESA CCI-LC [11]. The LULC product with the vegetation drought index can help evaluate the impact of drought on the ecosystem.

Vegetation drought indices are commonly used as proxies of productivity [25, 29]. The main environmental variables that affect productivity are water supply and demand [22]. Those are measured by precipitation and evapotranspiration (ET), commonly collected from weather stations. Usually, in developing countries (i.e., Chile), incomplete records or gaps present a challenge. But, there are satellite estimates of these variables. To evaluate drought, the World Meteorological Organization (WMO; [36]) has proposed the Standardized Precipitation Index (SPI; [19]), a multiscalar drought index, which has been used worldwide. For Chile, Zambrano et al. [41] derived and evaluated it from the product of the Climate Hazards Group InfraRed Precipitation with Station data (CHIRPS; [13]). For water demand, it is used ET. The vegetation biomass productivity is strongly related to ET [Steduto et al.]. The atmospheric evaporative demand (AED) represents the maximum ET rate from a land surface (without water restriction), also known as reference ET. The recommended method for its calculation is the FAO Penman-Monteith [26, 5]. Due to climate change, AED is increasing, driving ET rise [30]. But, it is not always true [21]. For example, regions where AET is highest have the lowest ET. The MOD16 product [Running, S and Mu, Q and Zhao, 24] provides AET and ET satellite estimates and has been used to derive drought indices [23]. Soil moisture (SM) is an Essential Climate Variable (ECV) that modulates vegetative growth. The climate change initiative (CCI) from the European Space Agency (ESA) delivers the ESA CCI SM product [10] (current version 6.1), which has been helpful to monitor drought [42]. Besides, total water storage can be retrieved by the Gravity Recovery and Climate Experiment (GRACE), which allows analyzing water availability changes [3, 18]. The water demand and supply by remote sensing can help evaluate how they have impacted vegetation productivity.

We aims to analyze the climate-induced water scarcity over continental Chile for 2000-2023 by using estimated environmental variables of biomass productivity, and water demand/supply gather from earth observation products. The specific objective for the study are i) to evaluate LULC change for 2001-2021, ii) to derive and assess the vegetation drought index zcNDVI as a proxy of biomass productivity, iii) analyze the interconnection of zcNDVI with drought indices of supply (i.e., precipitation), demand (i.e, ET), and vegetation cover; and iv) we will investigate if the observed changes are linked to the TWS and SM.

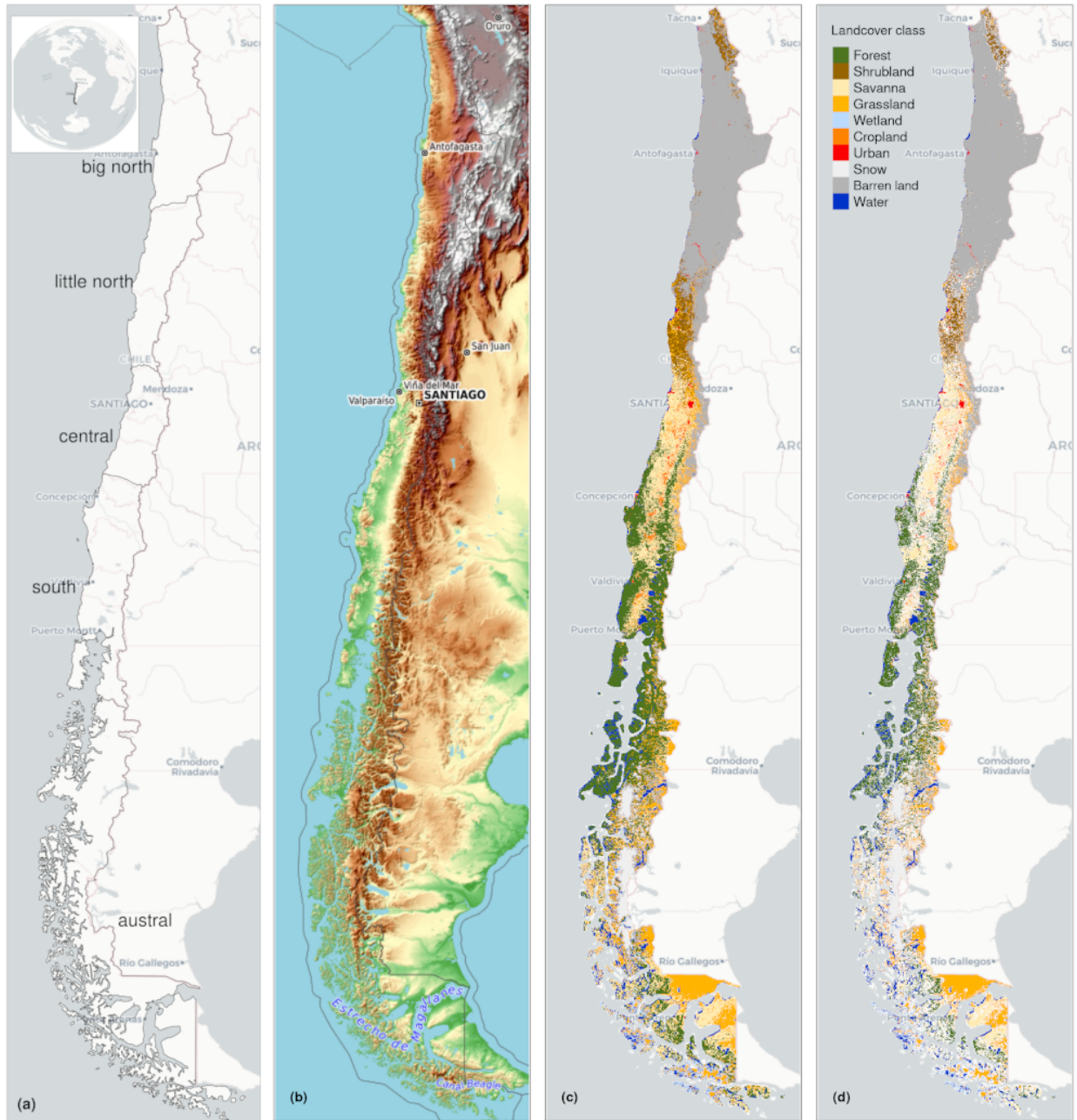


Figure 1: (a) Location of Central Chile and zones north (NCCH), central (CCCH), and south (SCCH) Central Chile. (b) Topography reference map. (c) Land cover classes for 2019. (d) Persistent land cover classes (> 80%) for 2001-2021.

## 2. Study area

## 3. Materials and Methods

### 3.1. Data

#### 3.1.1. Satellite data

#### 3.1.2. in-situ data

### 3.2. LULC change for 2001-2021

#### 3.2.1. Landcover change and persistence

### 3.3. Drought index for biomass productivity $zcNDVI$


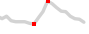




























### 3.4. Interconnection of productivity with drought indices of supply/demand and vegetation cover

### 3.5. Total water storage and Soil Moisture

## 4. Results

### 4.1. LULC change for 2001-2021

Table 1: Value of linear change trend next to time-series plot of surface, per landcover class (IGBP MCD12Q1.006) for 2001-2019 through Central Chile. Red dots on the plots indicate the maximum and minimum surface.

zone	Trend of change [ $km^2 year^{-1}$ ]					
	Shrubland	Savanna	Grassland	Barren land	Forest	Cropland
big north	-2.3 	0.1 	-31.2 	32.8 	NA 	NA 
little north	79.3 	-66.1 	-100.2 	104.0 	0.0 	-13.1 
central	130.2 	-128.6 	89.9 	23.3 	-66.2 	-24.4 
south	-14.6 	-316.2 	-55.9 	2.1 	412.4 	30.8 
austral	-44.6 	163.9 	226.1 	-80.2 	-9.1 	-1.0 

#### 4.1.1. Landcover change and persistence

### 4.2. Drought index for biomass productivity $zcNDVI$

### 4.3. Interconnection of productivity with drought indices of supply/demand and vegetation cover

### 4.4. Total water storage and Soil Moisture

## 5. Discussion

Authors should discuss the results and how they can be interpreted in perspective of previous studies and of the working hypotheses. The findings and their implications should be discussed in the broadest context possible. Future research directions may also be highlighted.

## 6. Conclusion

This section is not mandatory, but can be added to the manuscript if the discussion is unusually long or complex.

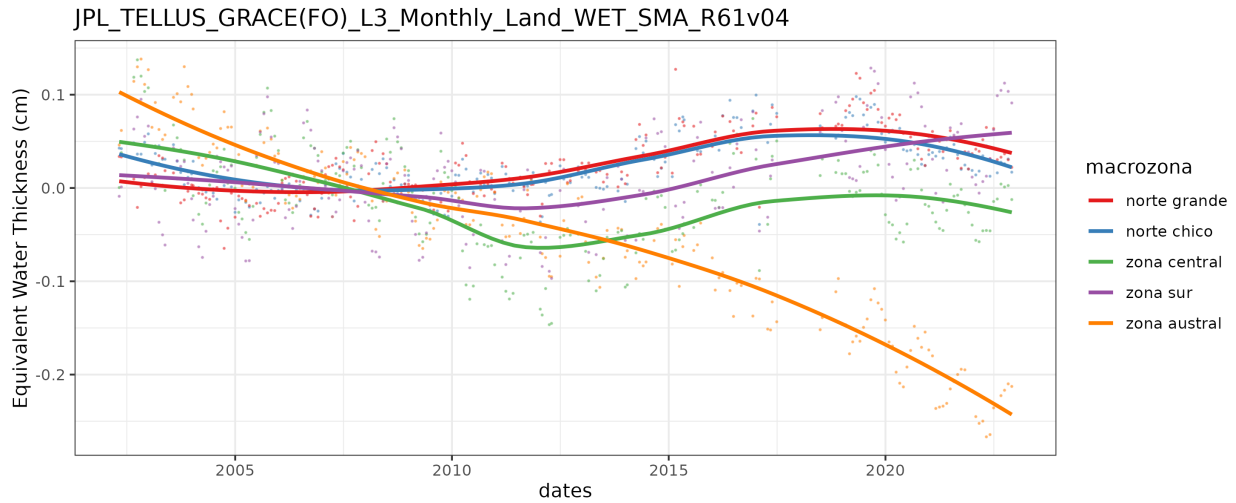


Figure 2: Total water storage (mm) trend for 2002-2023 in the five macrozones on continental Chile

## References

- [1] (2021). IPCC, 2021: Climate Change 2021: The Physical Science Basis. Contribution of Working Group I to the Sixth Assessment Report of the Intergovernmental Panel on Climate Change. *IPCC*.
- [2] AghaKouchak, A., Farahmand, A., Melton, F. S., Teixeira, J., Anderson, M. C., Wardlow, B. D., and Hain, C. R. (2015). Remote sensing of drought: Progress, challenges and opportunities. *Reviews of Geophysics*, 53(2):452–480.
- [3] Ahmed, M., Sultan, M., Wahr, J., and Yan, E. (2014). The use of GRACE data to monitor natural and anthropogenic induced variations in water availability across Africa. *Earth-Science Reviews*, 136:289–300.
- [4] Akinyemi, F. O. (2021). Vegetation Trends, Drought Severity and Land Use-Land Cover Change during the Growing Season in Semi-Arid Contexts. *Remote Sensing 2021, Vol. 13, Page 836*, 13(5):836.
- [5] Allen, R. G., Pruitt, W. O., Wright, J. L., Howell, T. A., Ventura, F., Snyder, R., Itenfisu, D., Steduto, P., Berengena, J., Yrisarry, J. B., Smith, M., Pereira, L. S., Raes, D., Perrier, A., Alves, I., Walter, I., and Elliott, R. (2005). reference ETo by the FAO56.
- [6] Boisier, J. P., Alvarez-Garretón, C., Cordero, R. R., Damiani, A., Gallardo, L., Garreaud, R. D., Lambert, F., Ramallo, C., Rojas, M., and Rondanelli, R. (2018). Anthropogenic drying in central-southern Chile evidenced by long-term observations and climate model simulations. *Elem Sci Anth*, 6(1):74.
- [7] Brown, J. F., Wardlow, B. D., Tadesse, T., Hayes, M. J., and Reed, B. C. (2008). The Vegetation Drought Response Index (VegDRI): A new integrated approach for monitoring drought stress in vegetation. *GIScience and Remote Sensing*, 45(1):16–46.
- [8] Cai, Z., Jönsson, P., Jin, H., and Eklundh, L. (2017). Performance of Smoothing Methods for Reconstructing NDVI Time-Series and Estimating Vegetation Phenology from MODIS Data. *Remote Sensing*, 9(12):1271.
- [9] Crausbay, S. D., Ramirez, A. R., Carter, S. L., Cross, M. S., Hall, K. R., Bathke, D. J., Betancourt, J. L., Colt, S., Cravens, A. E., Dalton, M. S., Dunham, J. B., Hay, L. E., Hayes, M. J., McEvoy, J., McNutt, C. A., Moritz, M. A., Nislow, K. H., Raheem, N., and Sanford, T. (2017). Defining Ecological Drought for the Twenty-First Century. *Bulletin of the American Meteorological Society*, 98(12):2543–2550.
- [10] Dorigo, W., Wagner, W., Albergel, C., Albrecht, F., Balsamo, G., Brocca, L., Chung, D., Ertl, M., Forkel, M., Gruber, A., Haas, E., Hamer, P. D., Hirschi, M., Ikonen, J., de Jeu, R., Kidd, R., Lahoz, W., Liu, Y. Y., Miralles, D., Mistelbauer, T., Nicolai-Shaw, N., Parinussa, R., Pratola, C., Reimer, C., van der Schalie, R., Seneviratne, S. I., Smolander, T., and Lecomte, P. (2017). ESA CCI Soil Moisture for improved Earth system understanding: State-of-the art and future directions. *Remote Sensing of Environment*, 203:185–215.
- [11] ESA (2017). Land Cover CCI Product User Guide Version 2. Technical report.
- [12] Friedl, M. and Sulla-Menashe, D. (2019). MCD12Q1 MODIS/Terra+Aqua Land Cover Type Yearly L3 Global 500m SIN Grid V006 [Data set]. NASA EOSDIS Land Processes DAAC.
- [13] Funk, C., Peterson, P., Landsfeld, M., Pedreros, D., Verdin, J., Shukla, S., Husak, G., Rowland, J., Harrison, L., Hoell, A., and Michaelsen, J. (2015). The climate hazards infrared precipitation with stations—a new environmental record for monitoring extremes. *Scientific Data* 2015 2:1, 2(1):1–21.
- [14] Garreaud, R., Alvarez-Garretón, C., Barichivich, J., Boisier, J. P., Christie, D., Galleguillos, M., LeQuesne, C., McPhee, J., and Zambrano-Bigiarini, M. (2017). The 2010-2015 mega drought in Central Chile: Impacts on regional hydroclimate and vegetation. *Hydrology and Earth System Sciences Discussions*, 2017:1–37.

- [15] IPCC (2013). *Climate Change 2013: The Physical Science Basis. Contribution of Working Group I to the Fifth Assessment Report of the Intergovernmental Panel on Climate Change*. Cambridge University Press, Cambridge, UK; New York, USA.
- [16] Kogan, F. N. (1990). Remote sensing of weather impacts on vegetation in non-homogeneous areas. *Int. J. Remote Sens.*, 11(8):1405–1419.
- [17] Kogan, F. N. (1995). Application of vegetation index and brightness temperature for drought detection. *Advances in Space Research*, 15(11):91–100.
- [18] Ma, S., Wu, Q., Wang, J., and Zhang, S. (2017). Temporal Evolution of Regional Drought Detected from GRACE TWSA and CCI SM in Yunnan Province, China. *Remote Sensing 2017, Vol. 9, Page 1124*, 9(11):1124.
- [19] Mckee, T. B., Doesken, N. J., and Kleist, J. (1993). The relationship of drought frequency and duration to time scales. In: *Proceedings of the Ninth Conference on Applied Climatology. American Meteorological Society*, (Boston):179–184.
- [20] Meroni, M., Rembold, F., Fasbender, D., and Vrieling, A. (2017). Evaluation of the Standardized Precipitation Index as an early predictor of seasonal vegetation production anomalies in the Sahel. *Remote Sensing Letters*, 8(4):301–310.
- [21] Milly, P. C. and Dunne, K. A. (2016). Potential evapotranspiration and continental drying. *Nature Climate Change*, 6(10):946–949.
- [22] Mishra, A. K., Ines, A. V., Das, N. N., Prakash Khedun, C., Singh, V. P., Sivakumar, B., and Hansen, J. W. (2015). Anatomy of a local-scale drought: Application of assimilated remote sensing products, crop model, and statistical methods to an agricultural drought study. *Journal of Hydrology*, 526:15–29.
- [23] Mu, Q., Zhao, M., Kimball, J. S., McDowell, N. G., and Running, S. W. (2013). A Remotely Sensed Global Terrestrial Drought Severity Index. *Bull. Amer. Meteor. Soc.*, 94(1):83–98.
- [24] Mu, Q., Zhao, M., and Running, S. W. (2011). Improvements to a MODIS global terrestrial evapotranspiration algorithm. *Remote Sensing of Environment*, 115(8):1781–1800.
- [25] Paruelo, J. M., Texeira, M., Staiano, L., Mastrángelo, M., Amdan, L., and Gallego, F. (2016). An integrative index of Ecosystem Services provision based on remotely sensed data. *Ecological Indicators*, 71:145–154.
- [26] Pereira, L. S., Allen, R. G., Smith, M., and Raes, D. (2015). Crop evapotranspiration estimation with FAO56: Past and future. *Agricultural Water Management*, 147:4–20.
- [27] Peters, A. J., Walter-Shea, E. A., Ji, L., Viña, A., Hayes, M., and Svoboda, M. D. (2002). Drought monitoring with NDVI-based Standardized Vegetation Index. *Photogrammetric Engineering and Remote Sensing*, 68(1):71–75.
- [Running, S and Mu, Q and Zhao] Running, S and Mu, Q and Zhao, M. MODIS/Terra Net Evapotranspiration 8-Day L4 Global 500m SIN Grid V061. 2021, distributed by NASA EOSDIS Land Processes DAAC.
- [29] Schucknecht, A., Meroni, M., Kayitakire, F., and Boureima, A. (2017). Phenology-Based Biomass Estimation to Support Rangeland Management in Semi-Arid Environments. *Remote Sensing 2017, Vol. 9, Page 463*, 9(5):463.
- [30] Seneviratne, S and Zhang, X and Adnan, M and Badi, W and Dereczynski, C and Luca, A and Ghosh, S and Iskandar, I and Kossin, J and Lewis, S and Otto, F and Pinto, I and Satoh, M and Vicente-Serrano, S and Wehner, M and Zhou ; Masson-Delmotte, B and V and, O. (2021). *Weather and Climate Extreme Events in a Changing Climate*. Cambridge University Press. In Press.
- [Steduto et al.] Steduto, P., Hsiao, T. C., Fereres, E., and Raes, D. Crop yield response to water.
- [32] Tran, H. T., Campbell, J. B., Wynne, R. H., Shao, Y., and Phan, S. V. (2019). Drought and Human Impacts on Land Use and Land Cover Change in a Vietnamese Coastal Area. *Remote Sensing 2019, Vol. 11, Page 333*, 11(3):333.
- [33] Vrieling, A., Meroni, M., Darvishzadeh, R., Skidmore, A. K., Wang, T., Zurita-Milla, R., Oosterbeek, K., O’Connor, B., and Paganini, M. (2018). Vegetation phenology from Sentinel-2 and field cameras for a Dutch barrier island. *Remote Sensing of Environment*, 215:517–529.
- [34] West, H., Quinn, N., and Horswell, M. (2019). Remote sensing for drought monitoring & impact assessment: Progress, past challenges and future opportunities. *Remote Sensing of Environment*, 232.
- [35] Wilhite, D. A. and Glantz, M. H. (1985). Understanding: The drought phenomenon: The role of definitions. *Water International*, 10(3):111–120.
- [36] WMO, Svoboda, M., Hayes, M., and Wood, D. A. (2012). *Standardized Precipitation Index User Guide*. Number 1090 in WMO. WMO, Geneva.
- [37] Younes, N., Joyce, K. E., and Maier, S. W. (2021). All models of satellite-derived phenology are wrong, but some are useful: A case study from northern Australia. *International Journal of Applied Earth Observation and Geoinformation*, 97:102285.
- [38] Zambrano, F. (2021). Four decades of satellite data for agricultural drought monitoring throughout the growing season in Central Chile. In *Drought*, volume Accepted. CRC Press.
- [39] Zambrano, F., Lillo-Saavedra, M., Verbist, K., and Lagos, O. (2016). Sixteen years of agricultural drought assessment of the BioBío region in Chile using a 250 m resolution vegetation condition index (VCI). *Remote Sensing*, 8(6):1–20.
- [40] Zambrano, F., Vrieling, A., Nelson, A., Meroni, M., and Tadesse, T. (2018). Prediction of drought-induced reduction of agricultural productivity in Chile from MODIS, rainfall estimates, and climate oscillation indices. *Remote Sensing of Environment*, 219:15–30.
- [41] Zambrano, F., Wardlow, B., Tadesse, T., Lillo-Saavedra, M., and Lagos, O. (2017). Evaluating satellite-derived long-term historical precipitation datasets for drought monitoring in Chile. *Atmospheric Research*, 186:26–42.
- [42] Zhang, L., Liu, Y., Ren, L., Jiang, S., Yang, X., Yuan, F., Wang, M., and Wei, L. (2019). Drought Monitoring and Evaluation by ESA CCI Soil Moisture Products over the Yellow River Basin. *IEEE Journal of Selected Topics in Applied Earth Observations and Remote Sensing*, 12(9):3376–3386.